

ROM2F/96/21
April, 1996

A Complete Analysis of FCNC and CP Constraints in General SUSY Extensions of the Standard Model

F. Gabbiani^a, E. Gabrielli^b, A. Masiero^c and L. Silvestrini^{d,b}

^a Department of Physics and Astronomy
University of Massachusetts, Amherst, MA 01003, USA

^b INFN, Sezione di Roma II,
Via della Ricerca Scientifica 1, I-00133 Roma, Italy.

^c Dip. di Fisica, Università di Perugia and
INFN, Sezione di Perugia, Via Pascoli, I-06100 Perugia, Italy.

^d Dipartimento di Fisica, Università di Roma “Tor Vergata”,
Via della Ricerca Scientifica 1, I-00133 Roma, Italy.

Abstract

We analyze the full set of constraints on gluino- and photino-mediated SUSY contributions to FCNC and CP violating phenomena. We use the mass insertion method, hence providing a model-independent parameterization which can be readily applied in testing extensions of the MSSM. In addition to clarifying controversial points in the literature, we provide a more exhaustive analysis of the CP constraints, in particular concerning ε'/ε . As physically meaningful applications of our analysis, we study the implications in SUSY-GUT’s and effective supergravities with flavour non-universality. This allows us to detail the domain of applicability and the correct procedure of implementation of the FC mass insertion approach.

1 Introduction

In looking for new physics beyond the electroweak Standard Model (SM) it is useful to regard the SM itself as an effective low energy theory valid up to some energy scale Λ at which the new physics sets in. One is then led to write all possible operators invariant under $SU(3) \otimes SU(2) \otimes U(1)$ using the fields of the SM. They can be organized according to their dependence on Λ . It is well known that as long as one writes operators not exceeding dimension four there are crucial conservations which automatically show up: baryon (B) and lepton (L) numbers and the absence of tree-level flavour changing neutral currents (FCNC). However, as soon as one proceeds beyond dimension four (i.e., one considers non-renormalizable operators which are suppressed by powers of Λ), these conservations are no longer automatically guaranteed. Either one has to choose large values for Λ (for instance, the grand unification or the Planck scale), or, if Λ is assumed to be not so far from the Fermi scale, additional constraints have to be imposed to play on the safe side in relation to B, L and FCNC violating processes.

Low energy supersymmetry (SUSY) [1] enters this latter class of models with new physics close enough to the Fermi scale. The problem of too violent B and L violations is more elegantly solved by the imposition of an additional discrete symmetry, the R-parity. As for the FCNC issue, given that now we are in the presence of new particles, the scalar partners of the fermions (sfermions) carrying flavour number, new constraints will have to be imposed to suppress operators of dimension greater than four, leading to potentially large FCNC rates. They amount to very severe limitations on the pattern of the sfermion mass matrices: they must be either very close to the unit matrix in flavour space (flavour universality) or almost proportional to the corresponding fermion mass matrices (alignment). Both universality or alignment can be either preset as kind of “initial” conditions [2, 3] or result from some dynamics of the theory [4, 5]. A very intense work on these different options has been going on recently, but, certainly, the flavour problem in SUSY remains quite an intriguing issue to be further explored.

Given a specific SUSY model it is in principle possible to make a full computation of all the FCNC (and, possibly, also CP violating) phenomena in that context. This is the case, for instance, of the minimal supersymmetric standard model (MSSM) where these detailed computations have led to the result of utmost importance that this model succeeds to pass unscathed all the severe FCNC and CP tests. However, given the variety of options that exist in extending the MSSM (for instance embedding it in some more fundamental theory at larger scales), it is important to have a way to extract from the whole host of FCNC and CP phenomena a set of upper limits on quantities which can be readily computed in any

chosen SUSY frame. Namely, one needs some kind of model-independent parameterization of the FCNC and CP quantities in SUSY to have an accessible immediate test of variants of the MSSM.

The best parameterization of this kind that has been proposed is in the framework of the so-called mass insertion approximation [6]. It concerns the most peculiar source of FCNC SUSY contributions that do not arise from the mere supersymmetrization of the FCNC in the SM. They originate from the FC couplings of gluinos and neutralinos to fermions and sfermions [7]. One chooses a basis for the fermion and sfermion states where all the couplings of these particles to neutral gauginos are flavour diagonal, while the FC is exhibited by the non-diagonality of the sfermion propagators. Denoting by Δ the off-diagonal terms in the sfermion mass matrices (i.e. the mass terms relating sfermion of the same electric charge, but different flavour), the sfermion propagators can be expanded as a series in terms of $\delta = \Delta/\tilde{m}^2$ where \tilde{m} is an average sfermion mass to be defined in more detail below. As long as Δ is significantly smaller than \tilde{m}^2 , we can just take the first term of this expansion and, then, the experimental information concerning FCNC and CP violating phenomena translates into upper bounds on these δ 's.

Obviously the above mass insertion method presents the major advantage that one does not need the full diagonalization of the sfermion mass matrices to perform a test of the SUSY model under consideration in the FCNC sector. It is enough to compute ratios of the off-diagonal over the diagonal entries of the sfermion mass matrices and compare the results with the general bounds on the δ 's that we provide here from all available experimental information.

There already exist two previous extensive analyses of this kind in the literature [8, 9]. Apart from the obvious improvements due to some progress in the FCNC and CP experimental results, we were motivated to perform this vast analysis by a twofold reason. On one hand, the two previous analyses differed in some results and, given the present interest in these kinds of bounds, it is important to clarify the controversial points. On the other hand, the quantities related to CP violation had not received enough attention in the previous works nor had significant flavour-conserving quantities (like the electric dipole moments of the neutron and of the electron or the radiative contributions to fermion masses) been computed in these analyses. Moreover, it is of interest to test this powerful mass insertion method in “realistic” sources of potentially large FCNC effects in SUSY, namely models with non-universal soft SUSY breaking terms and GUT extensions of the MSSM. In the final part of this work we will provide some examples of this kind of analyses. Some salient features of the present analysis are already contained in a work of ours [10]. Here we give a more exhaustive treatment of the previous results and we

enlarge our study to include physically relevant applications.

It is important to keep in mind that our analysis focuses only on the gluino- or photino-mediated FCNC contributions. It is well known that other SUSY sectors can yield relevant (and, sometimes, even dominant) contributions to FCNC. We refer to chargino or charged Higgs exchanges, in particular. However, the full computation of all these SUSY effects requires the full specification of the model. On the contrary, as we said, the spirit of our study is to provide a model-independent way to make a first check of the FCNC impact on classes of SUSY theories.

Before closing this introductory part, we provide some more details on the δ quantities on which we plan to set limits and on the procedure that is actually followed to derive such bounds.

There exist four different Δ mass insertions connecting flavours i and j along a sfermion propagator: $(\Delta_{ij})_{LL}$, $(\Delta_{ij})_{RR}$, $(\Delta_{ij})_{LR}$ and $(\Delta_{ij})_{RL}$. The indices L and R refer to the helicity of the fermion partners. The size of these Δ 's can be quite different. For instance, it is well known that in the MSSM case, only the LL mass insertion can change flavour, while all the other three above mass insertions are flavour conserving, i.e. they have $i = j$. In this case to realize a LR or RL flavour change one needs a double mass insertion with the flavour changed solely in a LL mass insertion and a subsequent flavour-conserving LR mass insertion. Even worse is the case of a FC RR transition: in the MSSM this can be accomplished only through a laborious set of three mass insertions, two flavour-conserving LR transitions and an LL FC insertion. Notice also that generally the Δ_{LR} quantity does not necessarily coincide with Δ_{RL} . For instance, in the MSSM and in several other cases, one flavour-conserving mass insertion is proportional to the mass of the corresponding right-handed fermion. Hence, $(\Delta_{ij})_{LR}$ and $(\Delta_{ij})_{RL}$ are proportional to the mass of the i -th and j -th fermion, respectively. We will comment further on this point later on in the paper. Instead of the dimensional quantities Δ it is more useful to provide bounds making use of dimensionless quantities, δ , that are obtained dividing the mass insertions by an average sfermion mass.

Concerning the definition of the average sfermion mass, in most cases it is indifferent how one exactly defines it (for instance, one can take half the sum of the two diagonal entries for the i -th and j -th sfermion). However, care must be taken when the degree of degeneracy of the sfermion is not so high (obviously in this case one has to check carefully that the whole mass insertion approach makes sense). Making quantitative checks it turned out that we were reproducing more closely the exact result, that is obtained by fully diagonalizing the sfermion mass matrices, by taking as a definition of average mass

between the sfermions m_1 and m_2 the quantity $\sqrt{m_1 m_2}$.

Finally an important point to underline is what we actually mean by using the experimental data in the derivation of the upper bounds on the δ 's. Clearly we have to take into account also the theoretical uncertainty in the SM in evaluating the different processes. For instance when considering the process $b \rightarrow s\gamma$ to derive the bounds on the δ_{23} quantities we consider as “experimental” input the interval $1 \times 10^{-4} < \text{BR}(b \rightarrow s\gamma) < 4 \times 10^{-4}$, which takes into account the still wide theoretical uncertainty in evaluating this BR within the SM. In any case, to avoid any ambiguity, for each process under consideration we will explicitly provide the “experimental” input that we use.

The paper is organized as follows. In Sect. 2 we analyze the bounds on the δ 's coming from $\Delta F = 2$ processes. After briefly summarizing the method of the effective hamiltonian that we make use of, we construct such effective hamiltonian for $\Delta S = 2$ transitions and we derive the corresponding bounds on the δ_{12} quantities for both the CP conserving and CP violating cases. We extend this analysis also to the D and B systems. Section 3 follows the same pattern of analysis as the previous one for the $\Delta F = 1$ processes. In particular we devote special attention to the evaluation of the bounds coming from the CP violating ε' quantity. A comment on the role played by the QCD corrections in our analysis is provided in Sect. 4. Then Sect. 5 compares the bounds that we derived for some δ quantities with their values in two classes of extensions of the MSSM which are actively investigated at the moment and that present important sources of FCNC. We refer to SUSY GUT's where not only are such large contributions to FCNC potentially present, but, at least if we can reliably trust the use of the Renormalization Group Equations (RGE's) in the evolution from the Planck to the GUT scale, they are indeed unavoidably there with important constraints on any such extension. The second class is given by models where the initial SUSY soft breaking terms lack the property of flavour universality. Although one can propose specific situations of SUSY breaking where these embarrassingly high contributions to FCNC are absent, it is certainly true that in the general case of supergravity models derived from four dimensional strings one expects such non-universality to be indeed present. Finally some conclusions and an outlook are presented in Sect. 6.

2 $\Delta F = 2$ processes

In this Section we will describe the calculation of the amplitude for $\Delta F = 2$ processes and we will present the phenomenological analysis of these transitions and the limits on

sfermion masses thereby obtained.

2.1 Effective Hamiltonian

Let us briefly recall the procedure to calculate the Effective Hamiltonian (EH) for a given process. One has to go through the following steps:

1. calculate the amplitude between quark and gluon states of definite momenta in the full theory;
2. choose a basis of local operators for the effective theory and calculate their matrix elements between the same states used in point 1;
3. determine the coefficients of the operators in the EH by matching the full theory with the effective one.

The matching is given by the following relation:

$$\langle f | S | i \rangle = -i \sum_j C_j \langle f | O_j | i \rangle , \quad (1)$$

where C_i are the Wilson coefficients and O_i the operators of the EH:

$$\mathcal{H}_{\text{EH}} = \sum_j C_j \mathcal{O}_j \quad (2)$$

Let us now specialize to the case of $\Delta S = 2$ processes. The amplitude in the full theory is given by the calculation of the diagrams in fig. 1. Having calculated the amplitude in the full theory, we now have to choose a basis of local operators and perform the matching. Our choice is the following:

$$\begin{aligned} Q_1 &= \bar{d}_L^\alpha \gamma_\mu s_L^\alpha \bar{d}_L^\beta \gamma^\mu s_L^\beta , \\ Q_2 &= \bar{d}_R^\alpha s_L^\alpha \bar{d}_R^\beta s_L^\beta , \\ Q_3 &= \bar{d}_R^\alpha s_L^\beta \bar{d}_R^\beta s_L^\alpha , \\ Q_4 &= \bar{d}_R^\alpha s_L^\alpha \bar{d}_L^\beta s_R^\beta , \\ Q_5 &= \bar{d}_R^\alpha s_L^\beta \bar{d}_L^\beta s_R^\alpha , \end{aligned} \quad (3)$$

plus the operators $\tilde{Q}_{1,2,3}$ obtained from the $Q_{1,2,3}$ by the exchange $L \leftrightarrow R$. Here $q_{R,L} = \frac{(1 \pm \gamma_5)}{2} q$, and α and β are colour indices. The colour matrices normalization is $\text{Tr}(t^A t^B) = \delta^{AB}/2$.

Performing the matching we obtain the following result for the $\Delta S = 2$ EH:

$$\begin{aligned}
\mathcal{H}_{\{ \{}} &= -\frac{\alpha_s^2}{216m_{\tilde{q}}^2} \left\{ \left(\delta_{12}^d \right)_{LL}^2 (24 Q_1 x f_6(x) + 66 Q_1 \tilde{f}_6(x)) \right. \\
&+ \left(\delta_{12}^d \right)_{RR}^2 (24 \tilde{Q}_1 x f_6(x) + 66 \tilde{Q}_1 \tilde{f}_6(x)) \\
&+ \left(\delta_{12}^d \right)_{LL} \left(\delta_{12}^d \right)_{RR} (504 Q_4 x f_6(x) - 72 Q_4 \tilde{f}_6(x) \\
&\quad + 24 Q_5 x f_6(x) + 120 Q_5 \tilde{f}_6(x)) \\
&+ \left(\delta_{12}^d \right)_{RL}^2 (204 Q_2 x f_6(x) - 36 Q_3 x f_6(x)) \\
&+ \left(\delta_{12}^d \right)_{LR}^2 (204 \tilde{Q}_2 x f_6(x) - 36 \tilde{Q}_3 x f_6(x)) \\
&\left. + \left(\delta_{12}^d \right)_{LR} \left(\delta_{12}^d \right)_{RL} (-132 Q_4 \tilde{f}_6(x) - 180 Q_5 \tilde{f}_6(x)) \right\}, \tag{4}
\end{aligned}$$

where $x = m_{\tilde{g}}^2/m_{\tilde{q}}^2$, $m_{\tilde{q}}$ is the average squark mass, $m_{\tilde{g}}$ is the gluino mass and the functions $f_6(x)$ and $\tilde{f}_6(x)$ are given by (we follow the notation of ref. [9]):

$$\begin{aligned}
f_6(x) &= \frac{6(1+3x) \ln x + x^3 - 9x^2 - 9x + 17}{6(x-1)^5}, \\
\tilde{f}_6(x) &= \frac{6x(1+x) \ln x - x^3 - 9x^2 + 9x + 1}{3(x-1)^5}. \tag{5}
\end{aligned}$$

This result is in agreement with ref. [11], but differs from ref. [9] in the Left-Right terms. In order to clarify these discrepancies, we explicitly give the contribution to the EH coming from the diagrams in fig. 1 in the case of Left-Right mass insertions:

$$\begin{aligned}
a) + b) &= \frac{\alpha_s^2}{216m_{\tilde{q}}^2} \left\{ \left[\left(\delta_{12}^d \right)_{RL}^2 (-252 Q_2 x f_6(x) - 12 Q_3 x f_6(x)) + L \leftrightarrow R \right] \right. \\
&+ \left. \left(\delta_{12}^d \right)_{LR} \left(\delta_{12}^d \right)_{RL} (12 Q_4 \tilde{f}_6(x) + 252 Q_5 \tilde{f}_6(x)) \right\}, \\
c) + d) &= \frac{\alpha_s^2}{216m_{\tilde{q}}^2} \left\{ \left[\left(\delta_{12}^d \right)_{RL}^2 (48 Q_2 x f_6(x) + 48 Q_3 x f_6(x)) + L \leftrightarrow R \right] \right. \\
&+ \left. \left(\delta_{12}^d \right)_{LR} \left(\delta_{12}^d \right)_{RL} (120 Q_4 \tilde{f}_6(x) - 72 Q_5 \tilde{f}_6(x)) \right\}. \tag{6}
\end{aligned}$$

Our results also differ from ref. [8]. To obtain our results, in eqs. (3.2 a) and c) of ref. [8] the terms proportional to the function $M(x)$ must be multiplied by the coefficient $(-1/2)$, while in eq. (3.2 b) the function $G(x)$ must be multiplied by (-1) .

2.2 Hadronic Matrix Elements

We now give the matrix elements of the operators Q_i between K mesons, in the vacuum insertion approximation (VIA). From PCAC we obtain the basic formulas:

$$\begin{aligned}\langle K^0 | \bar{d}^\alpha \gamma_\mu \gamma_5 s^\alpha | 0 \rangle \langle 0 | \bar{d}^\beta \gamma^\mu \gamma_5 s^\beta | \bar{K}^0 \rangle &= \frac{m_K f_K^2}{2} \\ \langle K^0 | \bar{d}^\alpha \gamma_5 s^\alpha | 0 \rangle \langle 0 | \bar{d}^\beta \gamma_5 s^\beta | \bar{K}^0 \rangle &= -\frac{m_K f_K^2}{2} \left(\frac{m_K}{m_s + m_d} \right)^2,\end{aligned}\quad (7)$$

where m_K is the mass of the K mesons and m_s , m_d are the masses of s and d quarks respectively. From eq. (7) we derive:

$$\begin{aligned}\langle K^0 | Q_1 | \bar{K}^0 \rangle &= \frac{1}{3} m_K f_K^2, \\ \langle K^0 | Q_2 | \bar{K}^0 \rangle &= -\frac{5}{24} \left(\frac{m_K}{m_s + m_d} \right)^2 m_K f_K^2, \\ \langle K^0 | Q_3 | \bar{K}^0 \rangle &= \frac{1}{24} \left(\frac{m_K}{m_s + m_d} \right)^2 m_K f_K^2, \\ \langle K^0 | Q_4 | \bar{K}^0 \rangle &= \left[\frac{1}{24} + \frac{1}{4} \left(\frac{m_K}{m_s + m_d} \right)^2 \right] m_K f_K^2, \\ \langle K^0 | Q_5 | \bar{K}^0 \rangle &= \left[\frac{1}{8} + \frac{1}{12} \left(\frac{m_K}{m_s + m_d} \right)^2 \right] m_K f_K^2,\end{aligned}\quad (8)$$

where we have set equal to one all the B parameters. Our results for the matrix elements in eq. (8) agree with ref. [11] but disagree with ref. [9] in the sign of the terms proportional to $(m_K/(m_s + m_d))^2$. This is probably due to a difference in the sign of the last line of eq. (7). We have checked that the sign we have obtained agrees with other previous calculations (see e.g. ref. [12]).

2.3 General Analysis of $\Delta F = 2$ Processes

We now present the results of a model-independent analysis of low energy $\Delta F = 2$ processes. Let us start from $K^0 - \bar{K}^0$ mixing. The $K_L - K_S$ mass difference Δm_K is given by:

$$\Delta m_K = 2 \operatorname{Re} \langle K^0 | \mathcal{H}_{\{\{ \}} | \tilde{\mathcal{K}}' \rangle. \quad (9)$$

Substituting the expressions (4) for the EH and (8) for the matrix elements into (9), we obtain the following expression for Δm_K :

$$\Delta m_K = -\frac{\alpha_s^2}{216 m_{\tilde{q}}^2} \frac{2}{3} m_K f_K^2 \left\{ \left(\delta_{12}^d \right)_{LL}^2 \left(24 x f_6(x) + 66 \tilde{f}_6(x) \right) \right\}$$

$$\begin{aligned}
& + \left(\delta_{12}^d \right)_{RR}^2 \left(24 x f_6(x) + 66 \tilde{f}_6(x) \right) \\
& + \left(\delta_{12}^d \right)_{LL} \left(\delta_{12}^d \right)_{RR} \left[\left(384 \left(\frac{m_K}{m_s + m_d} \right)^2 + 72 \right) x f_6(x) \right. \\
& \quad \left. + \left(-24 \left(\frac{m_K}{m_s + m_d} \right)^2 + 36 \right) \tilde{f}_6(x) \right] \\
& + \left(\delta_{12}^d \right)_{LR}^2 \left[-132 \left(\frac{m_K}{m_s + m_d} \right)^2 x f_6(x) \right] \\
& + \left(\delta_{12}^d \right)_{RL}^2 \left[-132 \left(\frac{m_K}{m_s + m_d} \right)^2 x f_6(x) \right] \\
& + \left. \left(\delta_{12}^d \right)_{LR} \left(\delta_{12}^d \right)_{RL} \left[-144 \left(\frac{m_K}{m_s + m_d} \right)^2 - 84 \right] \tilde{f}_6(x) \right\}. \quad (10)
\end{aligned}$$

Analogous expressions can be found for $D - \bar{D}$ and $B - \bar{B}$ mixing. Starting from eq. (10), and imposing that the contribution of each term in (10) does not exceed (in absolute value) the measured Δm_K , we obtain the limits on the δ 's reported in table 1, barring accidental cancellations. Here and in the following we take $(\delta_{ij})_{LR} \simeq (\delta_{ij})_{RL}$, to simplify the analysis¹. The parameters and upper limits used here and in the following are reported in tables 2 and 3. In the $K - \bar{K}$ system, limits can also be obtained from the CP-violating parameter ε : these are reported in table 4. The dependence of the limits in table 1 on x is given in figures 2, 3 and 4. The dependence of the limits in table 4 on x is identical.

3 $\Delta F = 1$ Processes

In this Section we will discuss the calculation of the EH for $\Delta F = 1$ transitions and the phenomenological analysis of these processes, following the outline of Section 2.

3.1 Effective Hamiltonian

In the full theory, there are two classes of diagrams contributing to $\Delta F = 1$ transitions: box diagrams (see fig. 5) and penguin diagrams (see fig. 6). In the case of gluino-mediated processes, these two contributions are of the same order and therefore must be included

¹As we said in the Introduction, this approximation does not hold true in general: for example, in the MSSM we have $(\delta_{12}^d)_{RL}/(\delta_{12}^d)_{LR} = m_d/m_s \ll 1$. However, as the amplitudes we study are Left-Right symmetric, the bounds that we find can be easily extended to the asymmetric case $(\delta_{ij})_{LR} \gg (\delta_{ij})_{RL}$ or $(\delta_{ij})_{LR} \ll (\delta_{ij})_{RL}$.

x	$\sqrt{ \text{Re}(\delta_{12}^d) ^2}$	$\sqrt{ \text{Re}(\delta_{12}^d) ^2}$	$\sqrt{ \text{Re}(\delta_{12}^d)_{LL}(\delta_{12}^d)_{RR} }$
0.3	1.9×10^{-2}	7.9×10^{-3}	2.5×10^{-3}
1.0	4.0×10^{-2}	4.4×10^{-3}	2.8×10^{-3}
4.0	9.3×10^{-2}	5.3×10^{-3}	4.0×10^{-3}

x	$\sqrt{ \text{Re}(\delta_{13}^d) ^2}$	$\sqrt{ \text{Re}(\delta_{13}^d) ^2}$	$\sqrt{ \text{Re}(\delta_{13}^d)_{LL}(\delta_{13}^d)_{RR} }$
0.3	4.6×10^{-2}	5.6×10^{-2}	1.6×10^{-2}
1.0	9.8×10^{-2}	3.3×10^{-2}	1.8×10^{-2}
4.0	2.3×10^{-1}	3.6×10^{-2}	2.5×10^{-2}

x	$\sqrt{ \text{Re}(\delta_{12}^u) ^2}$	$\sqrt{ \text{Re}(\delta_{12}^u) ^2}$	$\sqrt{ \text{Re}(\delta_{12}^u)_{LL}(\delta_{12}^u)_{RR} }$
0.3	4.7×10^{-2}	6.3×10^{-2}	1.6×10^{-2}
1.0	1.0×10^{-1}	3.1×10^{-2}	1.7×10^{-2}
4.0	2.4×10^{-1}	3.5×10^{-2}	2.5×10^{-2}

Table 1: Limits on $\text{Re}(\delta_{ij})_{AB}(\delta_{ij})_{CD}$, with $A, B, C, D = (L, R)$, for an average squark mass $m_{\tilde{q}} = 500\text{GeV}$ and for different values of $x = m_{\tilde{q}}^2/m_{\tilde{q}}^2$. For different values of $m_{\tilde{q}}$, the limits can be obtained multiplying the ones in the table by $m_{\tilde{q}}(\text{GeV})/500$.

Constants	Values
m_π	140 MeV
m_K	490 MeV
m_B	5.278 GeV
m_D	1.86 GeV
f_π	132 MeV
f_K	160 MeV
f_B	200 MeV
f_D	200 MeV
$\text{Re}A_0$	2.7×10^{-7} GeV
ω	0.045
τ_B	1.49×10^{-12} s
m_s	150 MeV
m_c	1.5 GeV
m_b	4.5 GeV
$\alpha_s(M_W)$	0.12
$ \mathbf{V}_{23} $	0.04
$ \mathbf{V}_{31} $	0.01

Table 2: Constants used in the phenomenological analysis.

Quantity	Value
Δm_K	$< 3.521 \times 10^{-12}$ MeV
ε	$< 2.268 \times 10^{-3}$
ε'/ε	$< 2.7 \times 10^{-3}$
Δm_B	$< 3.75 \times 10^{-10}$ MeV
Δm_D	$< 1.32 \times 10^{-10}$ MeV
$\text{BR}(b \rightarrow s\gamma)$	$(1 - 4) \times 10^{-4}$
$\text{BR}(\mu \rightarrow e\gamma)$	$< 4.9 \times 10^{-11}$
$\text{BR}(\tau \rightarrow e\gamma)$	$< 1.2 \times 10^{-4}$
$\text{BR}(\tau \rightarrow \mu\gamma)$	$< 4.2 \times 10^{-6}$
d_n	$< 11 \times 10^{-26}$ e cm
d_e	$< 7 \times 10^{-27}$ e cm

Table 3: Limits used in the phenomenological analysis.

x	$\sqrt{ \text{Im}(\delta_{12}^d)_{LL}^2 }$	$\sqrt{ \text{Im}(\delta_{12}^d)_{LR}^2 }$	$\sqrt{ \text{Im}(\delta_{12}^d)_{LL}(\delta_{12}^d)_{RR} }$
0.3	1.5×10^{-3}	6.3×10^{-4}	2.0×10^{-4}
1.0	3.2×10^{-3}	3.5×10^{-4}	2.2×10^{-4}
4.0	7.5×10^{-3}	4.2×10^{-4}	3.2×10^{-4}

Table 4: Limits on $\text{Im}(\delta_{12}^d)_{AB}(\delta_{12}^d)_{CD}$, with $A, B, C, D = (L, R)$, for an average squark mass $m_{\tilde{q}} = 500$ GeV and for different values of $x = m_{\tilde{q}}^2/m_q^2$. For different values of $m_{\tilde{q}}$, the limits can be obtained multiplying the ones in the table by $m_{\tilde{q}}(\text{GeV})/500$.

in the analysis. While there exist in the literature various calculations of the penguin contribution [13], there was no calculation of the box diagrams in fig. 5 before our analysis in ref. [10]. A complete basis for the $\Delta S = 1$ EH is the following:

$$\begin{aligned}
O_3 &= (\bar{d}_L^\alpha \gamma^\mu s_L^\alpha) \sum_{q=u,d,s} (\bar{q}_L^\beta \gamma_\mu q_L^\beta), \\
O_4 &= (\bar{d}_L^\alpha \gamma^\mu s_L^\beta) \sum_{q=u,d,s} (\bar{q}_L^\beta \gamma_\mu q_L^\alpha), \\
O_5 &= (\bar{d}_L^\alpha \gamma^\mu s_L^\alpha) \sum_{q=u,d,s} (\bar{q}_R^\beta \gamma_\mu q_R^\beta), \\
O_6 &= (\bar{d}_L^\alpha \gamma^\mu s_L^\beta) \sum_{q=u,d,s} (\bar{q}_R^\beta \gamma_\mu q_R^\alpha), \\
O_7 &= \frac{Q_d e}{8\pi^2} m_s \bar{d}_L^\alpha \sigma^{\mu\nu} s_R^\alpha F_{\mu\nu}, \\
O_8 &= \frac{g}{8\pi^2} m_s \bar{d}_L^\alpha \sigma^{\mu\nu} t_{\alpha\beta}^A s_R^\beta G_{\mu\nu}^A,
\end{aligned} \tag{11}$$

plus the operators \tilde{O}_i obtained from O_i by the exchange $L \leftrightarrow R$. Here $\sigma^{\mu\nu} = \frac{i}{2}[\gamma^\mu, \gamma^\nu]$, α and β are colour indices, g and e are the strong and electromagnetic couplings, $Q_d = -\frac{1}{3}$ and m_s is the mass of the strange quark. Evaluating the diagrams in figures 5 and 6, and performing the matching, we obtain the Wilson coefficients, which are given by:

$$\begin{aligned}
C_3 &= \frac{\alpha_s^2}{m_{\tilde{q}}^2} (\delta_{12}^d)_{LL} \left(-\frac{1}{9} B_1(x) - \frac{5}{9} B_2(x) - \frac{1}{18} P_1(x) - \frac{1}{2} P_2(x) \right), \\
C_4 &= \frac{\alpha_s^2}{m_{\tilde{q}}^2} (\delta_{12}^d)_{LL} \left(-\frac{7}{3} B_1(x) + \frac{1}{3} B_2(x) + \frac{1}{6} P_1(x) + \frac{3}{2} P_2(x) \right), \\
C_5 &= \frac{\alpha_s^2}{m_{\tilde{q}}^2} (\delta_{12}^d)_{LL} \left(\frac{10}{9} B_1(x) + \frac{1}{18} B_2(x) - \frac{1}{18} P_1(x) - \frac{1}{2} P_2(x) \right), \\
C_6 &= \frac{\alpha_s^2}{m_{\tilde{q}}^2} (\delta_{12}^d)_{LL} \left(-\frac{2}{3} B_1(x) + \frac{7}{6} B_2(x) + \frac{1}{6} P_1(x) + \frac{3}{2} P_2(x) \right), \\
C_7 &= \frac{\alpha_s \pi}{m_{\tilde{q}}^2} \left[(\delta_{12}^d)_{LL} \frac{8}{3} M_3(x) + (\delta_{12}^d)_{LR} \frac{m_{\tilde{g}}}{m_s} \frac{8}{3} M_1(x) \right], \\
C_8 &= \frac{\alpha_s \pi}{m_{\tilde{q}}^2} \left[(\delta_{12}^d)_{LL} \left(-\frac{1}{3} M_3(x) - 3 M_4(x) \right) \right. \\
&\quad \left. + (\delta_{12}^d)_{LR} \frac{m_{\tilde{g}}}{m_s} \left(-\frac{1}{3} M_1(x) - 3 M_2(x) \right) \right],
\end{aligned} \tag{12}$$

where again the coefficients \tilde{C}_i can be obtained from the C_i just by the exchange $L \leftrightarrow R$. The functions $B_i(x)$ which result from the calculation of the box diagrams are given by:

$$\begin{aligned}
B_1(x) &= \frac{1 + 4x - 5x^2 + 4x \ln(x) + 2x^2 \ln(x)}{8(1-x)^4}, \\
B_2(x) &= x \frac{5 - 4x - x^2 + 2 \ln(x) + 4x \ln(x)}{2(1-x)^4},
\end{aligned} \tag{13}$$

while the functions P_i and M_i , obtained from the gluino penguins, are:

$$\begin{aligned}
P_1(x) &= \frac{1 - 6x + 18x^2 - 10x^3 - 3x^4 + 12x^3 \ln(x)}{18(x-1)^5}, \\
P_2(x) &= \frac{7 - 18x + 9x^2 + 2x^3 + 3\ln(x) - 9x^2 \ln(x)}{9(x-1)^5}, \\
M_1(x) &= 4B_1(x), \\
M_2(x) &= -x B_2(x), \\
M_3(x) &= \frac{-1 + 9x + 9x^2 - 17x^3 + 18x^2 \ln(x) + 6x^3 \ln(x)}{12(x-1)^5}, \\
M_4(x) &= \frac{-1 - 9x + 9x^2 + x^3 - 6x \ln(x) - 6x^2 \ln(x)}{6(x-1)^5}.
\end{aligned} \tag{14}$$

Our results for the gluino penguins coincide with the results of ref. [9].

3.2 Hadronic Matrix Elements

We report here for completeness the relevant matrix elements of operators O_{3-7} , which can be found in ref. [14]:

$$\begin{aligned}
\langle(\pi\pi)_{I=0}|O_3|K\rangle &= \frac{X}{12}, \\
\langle(\pi\pi)_{I=0}|O_4|K\rangle &= \frac{X}{4}, \\
\langle(\pi\pi)_{I=0}|O_5|K\rangle &= -\frac{Z}{12}, \\
\langle(\pi\pi)_{I=0}|O_6|K\rangle &= -\frac{Z}{4}, \\
\langle(\pi\pi)_{I=0}|O_8|K\rangle &= -\frac{1}{16\pi^2} \frac{11}{2} \frac{f_K^2}{f_\pi^3} m_K^2 m_\pi^2, \\
\langle(\pi\pi)_{I=2}|O_i|K\rangle &= 0 \quad i = 3, \dots, 6,
\end{aligned} \tag{15}$$

where

$$\begin{aligned}
X &= f_\pi (m_K^2 - m_\pi^2), \\
Z &= 4 \left(\frac{f_K}{f_\pi} - 1 \right) f_\pi \left(\frac{m_K^2}{m_s + m_d} \right)^2.
\end{aligned} \tag{16}$$

The matrix elements of the operators \tilde{O}_i can be obtained from the matrix elements of O_i multiplying them by (-1) .

3.3 General Analysis of $\Delta F = 1$ Processes

We now present the results of a model-independent analysis of $\Delta F = 1$ processes. We will start with $\Delta S = 1$ transitions, and in particular with the CP-violating parameter ε'/ε , then we proceed to $\Delta B = 1$ and consider radiative B decays, and continue with the constraints coming from radiative decays in the leptonic sector: $\mu \rightarrow e\gamma$, $\tau \rightarrow \mu\gamma$ and $\tau \rightarrow e\gamma$. We will close this Section with limits on flavour-diagonal Left-Right mass terms coming from electric dipole moments and from radiative corrections to masses.

The expression for ε' is the following (see for example ref. [14]):

$$\varepsilon' = i \frac{e^{i(\delta_2 - \delta_0)}}{\sqrt{2}} \frac{\omega}{\text{Re } A_0} (\omega^{-1} \text{Im } A_2 - \text{Im } A_0) , \quad (17)$$

where $\omega = \text{Re } A_2 / \text{Re } A_0$, and the amplitudes are defined as:

$$A_I e^{i\delta_I} = \langle \pi\pi(I) | \mathcal{H}_{\text{eff}} | \mathcal{K}' \rangle , \quad (18)$$

where $I = 0, 2$ is the isospin of the final two-pion state and the δ_I 's are the strong phases induced by final-state interaction.

Imposing that the supersymmetric contribution to ε'/ε does not exceed in absolute value the upper limit in table 3, we obtain the conservative limits given in table 5. It is interesting to note that the contributions of box and penguin diagrams to the LL terms in (17), which are separately plotted in figs. 7 and 8 respectively, have opposite signs and therefore tend to cancel each other in the region around $x = 1$, where they are of the same size. This is the reason of the peak around $x = 1$ in the plot of the complete contribution, given in fig. 9.

A comment is necessary at this point. In the SM, the contribution to ε' coming from electropenguin operators is non-negligible for a heavy top. One might therefore wonder whether this remains true in SUSY or not. In particular, we have considered the contribution to ε' coming from gluino-mediated electroweak penguins.

Let us first note that gluino-mediated Z^0 -penguins are suppressed by a factor of m_s/M_Z , relative to γ -penguins [15]. This is due to the fact that the effective $b - s - Z$ vertex is proportional, in the case of gluino-mediated transitions, to the effective $b - s - \gamma$ vertex, apart from chirality breaking terms of order m_s . Now, for gauge invariance, the effective $b - s - \gamma$ vertex must be proportional either to $(\gamma_\mu q^2 - q_\mu q_\mu)$ or to $m_s \sigma_{\mu\nu} q^\nu$. The first form factor is the one which originates the so-called electropenguin operators. In the case of the photon, the q^2 factor cancels the pole of the propagator, giving an effective four-fermion operator, while in the case of the Z boson we get a suppression of order q^2/M_Z^2 which

x	$ \text{Im}(\delta_{12}^d)_{LL} $	$ \text{Im}(\delta_{12}^d)_{LR} $
0.3	1.0×10^{-1}	1.1×10^{-5}
1.0	4.8×10^{-1}	2.0×10^{-5}
4.0	2.6×10^{-1}	6.3×10^{-5}

Table 5: Limits from $\varepsilon'/\varepsilon < 2.7 \times 10^{-3}$ on $\text{Im}(\delta_{12}^d)$, for an average squark mass $m_{\tilde{q}} = 500\text{GeV}$ and for different values of $x = m_{\tilde{g}}^2/m_{\tilde{q}}^2$. For different values of $m_{\tilde{q}}$, the limits can be obtained multiplying the ones in the table by $(m_{\tilde{q}}(\text{GeV})/500)^2$.

makes these contributions negligible. We are thus left with the chirality breaking terms, which are themselves of order m_s/M_Z , and therefore can be safely neglected.

The contribution to ε' coming from gluino-mediated γ -superpenguins has got no explicit suppression factor: however, we have numerically checked that this contribution is negligible.

We now consider the decay $b \rightarrow s\gamma$. The gluino-mediated contribution is given by (see ref. [8]):

$$\text{BR}(b \rightarrow s\gamma) = \frac{\alpha_s^2 \alpha}{81\pi^2 m_{\tilde{q}}^4} m_b^3 \tau_B \left\{ \left| m_b M_3(x) \left(\delta_{23}^d \right)_{LL} \right. \right. \\ \left. \left. + m_{\tilde{g}} M_1(x) \left(\delta_{23}^d \right)_{LR} \right|^2 + L \leftrightarrow R \right\}. \quad (19)$$

Using the result (19) we can obtain the limits in table 6, by imposing that each individual term in eq. (19) does not exceed in absolute value the range given in tab. 3, which includes the uncertainty coming from the SM prediction. Table 6 shows that the decay $(b \rightarrow s + \gamma)$ does not limit the $(\delta_{23}^d)_{LL}$ insertion for a SUSY breaking of $O(500 \text{ GeV})$. Indeed, even taking $m_{\tilde{q}} = 100\text{GeV}$, the term $(\delta_{23}^d)_{LL}$ is only marginally limited ($(\delta_{23}^d)_{LL} < 0.3$ for $x = 1$). Obviously, $(\delta_{23}^d)_{LR}$ is much more constrained since with a δ_{LR} FC mass insertion the helicity flip needed for $(b \rightarrow s + \gamma)$ is realized in the gluino internal line and so this contribution has an amplitude enhancement of a factor $m_{\tilde{g}}/m_b$ over the previous case with δ_{LL} .

A similar analysis can be performed in the leptonic sector where the masses $m_{\tilde{q}}$ and $m_{\tilde{g}}$ are replaced by the average slepton mass $m_{\tilde{l}}$ and the photino mass $m_{\tilde{\gamma}}$ respectively.

x	$ \left(\delta_{23}^d\right)_{LL} $	$ \left(\delta_{23}^d\right)_{LR} $
0.3	4.4	1.3×10^{-2}
1.0	8.2	1.6×10^{-2}
4.0	26	3.0×10^{-2}

Table 6: Limits on the $|\delta_{23}^d|$ from $b \rightarrow s\gamma$ decay for an average squark mass $m_{\tilde{q}} = 500\text{GeV}$ and for different values of $x = m_{\tilde{g}}^2/m_{\tilde{q}}^2$. For different values of $m_{\tilde{q}}$, the limits can be obtained multiplying the ones in the table by $(m_{\tilde{q}}(\text{GeV})/500)^2$.

The branching ratio for the process $l_i \rightarrow l_j \gamma$ is the following (see ref. [8]):

$$\begin{aligned} \text{BR}(l_i \rightarrow l_j \gamma) = & \frac{\alpha^3}{G_F^2} \frac{12\pi}{m_l^4} \left\{ \left| M_3(x) \left(\delta_{ij}^l\right)_{LL} \right. \right. \\ & \left. \left. + \frac{m_{\tilde{\gamma}}}{m_l} M_1(x) \left(\delta_{ij}^l\right)_{LR} \right|^2 + L \leftrightarrow R \right\} \cdot \text{BR}(l_i \rightarrow l_j \nu_i \bar{\nu}_j). \end{aligned} \quad (20)$$

In table 7 we exhibit the bounds on $\left(\delta_{ij}^l\right)_{LL}$ and $\left(\delta_{ij}^l\right)_{LR}$ coming from the limits on $\mu \rightarrow e\gamma$, $\tau \rightarrow e\gamma$ and $\tau \rightarrow \mu\gamma$, for a slepton mass of $\mathcal{O}(100\text{ GeV})$ and for different values of $x = m_{\tilde{\gamma}}^2/m_{\tilde{l}}^2$. The dependence of those limits on x is given in fig. 11 and 12. Our results confirm those obtained in refs [8, 9].

We conclude this Section with the analysis of the limits on flavour-conserving $(\delta_{ii})_{LR}$ mass insertions coming from radiative corrections to mass terms and electric dipole moments².

A Left-Right diagonal mass insertion $(\delta_{ii})_{LR} = (\delta_{ii})_{RL}$ generates a one-loop mass term given by

$$\Delta m_i = -\frac{4}{3} \frac{2\alpha_s}{4\pi} m_{\tilde{g}} \text{Re} (\delta_{ii}^q)_{LR} I(x) \quad (21)$$

for quarks, and by

$$\Delta m_i = -\frac{2\alpha}{4\pi} m_{\tilde{\gamma}} \text{Re} (\delta_{ii}^l)_{LR} I(x) \quad (22)$$

for leptons. The function $I(x)$ is given by

$$I(x) = \frac{-1 + x - x \ln(x)}{(1-x)^2}. \quad (23)$$

²We thank R. Barbieri for suggesting this point to us.

x	$ \left(\delta_{12}^l\right)_{LL} $	$ \left(\delta_{12}^l\right)_{LR} $
0.3	4.1×10^{-3}	1.4×10^{-6}
1.0	7.7×10^{-3}	1.7×10^{-6}
5.0	3.2×10^{-2}	3.8×10^{-6}

x	$ \left(\delta_{13}^l\right)_{LL} $	$ \left(\delta_{13}^l\right)_{LR} $
0.3	15	8.9×10^{-2}
1.0	29	1.1×10^{-1}
5.0	1.2×10^2	2.4×10^{-1}

x	$ \left(\delta_{23}^l\right)_{LL} $	$ \left(\delta_{23}^l\right)_{LR} $
0.3	2.8	1.7×10^{-2}
1.0	5.3	2.0×10^{-2}
5.0	22	4.4×10^{-2}

Table 7: Limits on the $|\delta_{ij}^d|$ from $l_j \rightarrow l_i \gamma$ decays for an average slepton mass $m_{\tilde{l}} = 100\text{GeV}$ and for different values of $x = m_{\tilde{\gamma}}^2/m_{\tilde{l}}^2$. For different values of $m_{\tilde{l}}$, the limits can be obtained multiplying the ones in the table by $(m_{\tilde{l}}(\text{GeV})/100)^2$.

x	$ \text{Re}(\delta_{11}^d)_{LR} $	$ \text{Re}(\delta_{22}^d)_{LR} $	$ \text{Re}(\delta_{33}^d)_{LR} $
0.3	2.1×10^{-3}	3.1×10^{-2}	9.6×10^{-1}
1.0	1.6×10^{-3}	2.4×10^{-2}	7.3×10^{-1}
4.0	1.4×10^{-3}	2.1×10^{-2}	6.5×10^{-1}

x	$ \text{Re}(\delta_{11}^l)_{LR} $	$ \text{Re}(\delta_{22}^l)_{LR} $	$ \text{Re}(\delta_{33}^l)_{LR} $
0.3	1.1×10^{-2}	2.1	36
1.0	8.0×10^{-3}	1.6	27
5.0	7.1×10^{-3}	1.4	24

Table 8: Limits on $\text{Re}(\delta_{ii})_{LR}$ from one-loop mass terms, for $m_{\tilde{q}} = 500$ GeV and $m_{\tilde{l}} = 100$ GeV.

x	$ \text{Im}(\delta_{11}^d)_{LR} $	$ \text{Im}(\delta_{11}^u)_{LR} $	$ \text{Im}(\delta_{11}^l)_{LR} $
0.3	2.4×10^{-6}	4.9×10^{-6}	3.0×10^{-7}
1.0	3.0×10^{-6}	5.9×10^{-6}	3.7×10^{-7}
4.0	5.6×10^{-6}	1.1×10^{-5}	7.0×10^{-7}

Table 9: Limits on $\text{Im}(\delta_{ii})_{LR}$ from electric dipole moments, for $m_{\tilde{q}} = 500$ GeV and $m_{\tilde{l}} = 100$ GeV.

Imposing that these mass terms do not exceed in absolute value the masses of quarks and leptons (for the d quark we have used a value of 10 MeV), we obtain the limits given in table 8.

Limits on the imaginary parts of $(\delta_{ii})_{LR}$ can be obtained by analyzing the contribution to the Electric Dipole Moments (EDM) of the neutron and of the electron. The EDM of the electron and of u and d quarks are given by:

$$\begin{aligned}\frac{d_e}{e} &= -\frac{\alpha m_{\tilde{\gamma}}}{2\pi m_{\tilde{l}}^2} M_1(x) \operatorname{Im}(\delta_{11}^l)_{LR}, \\ \frac{d_d}{e} &= -\frac{2}{9} \frac{\alpha_s m_{\tilde{q}}}{\pi m_{\tilde{q}}^2} M_1(x) \operatorname{Im}(\delta_{11}^d)_{LR}, \\ \frac{d_u}{e} &= \frac{4}{9} \frac{\alpha_s m_{\tilde{q}}}{\pi m_{\tilde{q}}^2} M_1(x) \operatorname{Im}(\delta_{11}^u)_{LR}\end{aligned}\quad (24)$$

and in the quark model the EDM of the neutron is given by

$$d_n = \frac{1}{3} (4d_d - d_u). \quad (25)$$

Imposing that each of the above contributions does not exceed in absolute value the limits in table 3, we obtain the upper bounds in table 9.

The limits obtained from mass terms and EDM's are limits on diagonal terms, not on flavour-violating ones. However, in general one expects that off-diagonal terms should be proportional to diagonal ones via some (small) mixing angle, and therefore the limits above might be interpreted as indirect upper bounds on flavour violating terms.

If one compares the constraints in tables 8 and 9 with the bounds on the FC δ 's involving the first two generations, one notices that only the bound on $\operatorname{Im}(\delta_{11}^d)_{LR}$ is more severe than the corresponding limit on $\operatorname{Im}(\delta_{12}^d)_{LR}$. This means that if we envisage a situation where the diagonal entries are larger than the corresponding off-diagonal entries there is no chance to obtain a large contribution to ε'/ε from SUSY while respecting the constraint from d_n .

4 QCD corrections

In the framework of the Standard Model (SM), strong interactions are known to give sizeable contributions to FCNC processes, and in particular to $b \rightarrow s\gamma$ decays and to ε'/ε . It is therefore important to know whether QCD corrections could be so important also in our case, and how could the inclusion of these corrections modify the limits we previously obtained.

Let us start by considering $b \rightarrow s\gamma$ decays. In the SM the effect of QCD corrections is a dramatic enhancement of the rate, of a factor $\sim 2 - 5$ [16]. This is due to the mixing between the magnetic moment operator O_7 and the four fermion operator $O_2 = \bar{s}_L^\alpha \gamma_\mu c_L^\alpha \bar{c}_L^\beta \gamma^\mu b_L^\beta$, whose coefficient at the scale M_W is ~ 10 times bigger.

Since the mixing with O_8 is much smaller, we can use the following approximation for the coefficient of the operator O_7 at a scale $\mu \sim m_b$ [17]:

$$C_7(\mu) \simeq \eta^{\frac{16}{23}} C_7(M_W) + C_2(M_W) \sum_{i=1}^8 h_i \eta^{\alpha_i}, \quad (26)$$

where $\eta = \alpha_s(M_W)/\alpha_s(\mu)$ and h_i and α_i are related to the anomalous dimensions of the operators O_i .

Now we note that the last term in the r.h.s. of eq. (26), which is responsible for the enhancement, remains exactly the same when we include supersymmetric contributions. Indeed, gluino-mediated transitions only affect $C_7(M_W)$ in eq. (26). Therefore, if one takes into account the prediction of the standard model, including QCD corrections, when comparing the SUSY contributions due to gluino exchange with the experimental value for the decay $b \rightarrow s\gamma$, there is no need to explicitly consider QCD corrections to the SUSY contributions.

Of course, as previously noticed, one should bear in mind that to calculate the full amplitude for $b \rightarrow s\gamma$ decays in any definite SUSY model, one should include all SUSY contributions (chargino and neutralino mediated) and SM ones, and consider possible interference effects and cancellations [15, 18].

Concerning ε'/ε , one has to note two main points:

1. the constraints from ε' dominate over the ones from ε only in the LR sector, where just the magnetic moment operator contributes, and for the reasons given above QCD corrections are negligible in this case;
2. in the LL and RR sectors the main contribution to ε' in the strong sector is given by the operator O_6 . Numerically, we find that the effect of leading order QCD corrections is to enhance its coefficient by a factor ≤ 2 . This means that even with the inclusion of QCD corrections the dominant constraints in the LL and RR sectors come from ε . Therefore, the results of our analysis remain unaffected.

5 FCNC in SUSY-GUT's and in SUSY with Non-Universal Soft Breaking Terms

In this Section we consider two classes of SUSY theories with potentially interesting (or dangerous, according to the viewpoint) contributions to FCNC.

The first class includes GUT extensions of the MSSM where the presence of quark and lepton superfields in common supermultiplets and the large value of the top Yukawa coupling produce very conspicuous contributions, in particular in the leptonic sector.

The second class comprises models where the breaking of SUSY gives rise to soft breaking terms which are not flavour-universal. This is a common feature of effective supergravities that are the point-like limit of four-dimensional superstrings. Only with rather specific assumptions on the mechanism of SUSY breaking can one avoid the occurrence of such non-universality.

Obviously, there already exist rather exhaustive analyses of both these classes of SUSY theories in relation to the FCNC problem. It is not our purpose here to produce yet another analysis of this kind, but, rather, we intend to estimate the values of some δ mass insertions in a few examples within the two above-mentioned classes of generalized SUSY theories and to compare them with the bounds on the δ 's that we derived in the previous Sections. An interesting aspect of our analysis will be the comparison with the “exact” results that have been obtained in the literature using the physical (mass eigenstates) basis for fermions and sfermions. We will discuss to what extent the mass insertion approach is valid and how it has to be correctly implemented to get results which are quite close to the full computation in the mass eigenstate basis.

5.1 SUSY SU(5)

It has been known since the pioneering works of Duncan and Donoghue, Nilles and Wyler in 1983 [7] that even in the MSSM the running of sfermion masses from the superlarge scale where SUSY is broken down to the Fermi scale is responsible for a misalignment of fermion and sfermion mass matrices with the consequent presence of FC in $\tilde{g} - f - \tilde{f}$ or $\tilde{\gamma} - f - \tilde{f}$ vertices.

The key-feature of the unification of quark and lepton superfields into larger multiplets in SUSY-GUT's in relation to the FCNC issue was thoroughly investigated by Hall, Kostelecky and Rabi ten years ago [6]. But it was only recently, with the realization of the large size of the top Yukawa coupling, that it became clear that in SUSY-GUT's

radiative corrections can lead to slepton non-degeneracies so important as to imply L_e and L_μ violations just in the ballpark of the present or near future experimental range [19].

The interested reader can find all the details of this relevant low-energy manifestation of grand unification in the works of refs. [20, 21]. Here we limit ourselves to a computation of $\text{BR}(\mu \rightarrow e\gamma)$ in SUSY SU(5) using the mass insertion approximation. As we will see some of the δ quantities in SU(5) turn out to be only one order of magnitude smaller than the corresponding upper bounds that we found in Sect. 3 when analyzing the bounds coming from $\text{BR}(\mu \rightarrow e\gamma)$.

We follow closely the notation of ref. [20] where further details can be found. Denoting with T and \bar{F} the $\underline{10}$ and $\underline{\bar{5}}$ representations of SU(5) of standard matter and with H and \bar{H} the $\underline{5}$ and $\underline{\bar{5}}$ Higgs supermultiplets, the superpotential reads:

$$W = T_i \lambda_{ij}^u T_j H + T_i \lambda_{ij}^d \bar{F}_j \bar{H} \equiv T^T \boldsymbol{\lambda}^u T H + T^T \boldsymbol{\lambda}^d \bar{F} \bar{H}, \quad (27)$$

from the Planck scale down to the grand unification scale M_G . The scalar soft breaking terms, above M_G , are given by:

$$V_{\text{soft}} = \tilde{T}^\dagger \mathbf{m}_T^2 \tilde{T} + \tilde{\bar{F}}^\dagger \mathbf{m}_{\bar{F}}^2 \tilde{\bar{F}} + m_H^2 |H|^2 + m_{\bar{H}}^2 |\bar{H}|^2 + \tilde{T}^T \mathbf{A}^u \boldsymbol{\lambda}^u \tilde{T} H + \tilde{T}^T \mathbf{A}^d \boldsymbol{\lambda}^d \tilde{\bar{F}} \bar{H}. \quad (28)$$

Universality at the Planck scale is assumed:

$$\begin{aligned} \mathbf{m}_T^2 &= \mathbf{m}_{\bar{F}}^2 = m_0^2 \mathbb{I}, \\ m_H^2 &= m_{\bar{H}}^2 = m_0^2, \\ \mathbf{A}^u &= \mathbf{A}^d = A_0 \mathbb{I}. \end{aligned} \quad (29)$$

By solving the RGE's, one finds at M_G [20]:

$$\begin{aligned} \mathbf{m}_{TG}^2 &= \text{diag}(m_{TG}^2, m_{TG}^2, m_{TG}^2 - I_G) \equiv m_{TG}^2 \mathbb{I} - \mathbf{I}_G, \\ \mathbf{A}_G^d &= \text{diag}(A_{dG}, A_{dG}, A_{dG} - \frac{1}{3} I'_G) \equiv A_{dG} \mathbb{I} - \frac{1}{3} \mathbf{I}'_G, \\ \mathbf{A}_G^u &= \text{diag}(A_{uG} - \frac{1}{3} I'_G, A_{uG} - \frac{1}{3} I'_G, A_{uG} - I'_G), \\ \mathbf{m}_{\bar{F}G}^2 &= m_{\bar{F}G}^2 \mathbb{I}, \\ \boldsymbol{\lambda}_G^u &= \text{diag}(\lambda_{uG}, \lambda_{cG}, \lambda_{tG}), \end{aligned} \quad (30)$$

whereas $\boldsymbol{\lambda}^d$ gets renormalized to $\boldsymbol{\lambda}_G^d$. The explicit expression of all the quantities appearing in eq. (30) can be found in ref. [20]. From this computation one sees that the large value of the top Yukawa coupling, λ_t , produces major effects on the non-universality of the soft breaking terms after renormalizing them from M_{Pl} to M_G .

After SU(5) breaking one obtains the following slepton and lepton mass matrices at the scale M_Z :

$$-\mathcal{L}_{\mathcal{L}}^{\text{sl}} = \mathcal{L}^{\dagger} \mathbf{m}_{\mathcal{L}}^{\text{e}} \mathcal{L} + \mathcal{L}^{\dagger} \mathbf{m}_{\mathcal{L}}^{\text{d}} \mathcal{L} + \mathcal{L}^{\dagger} \mathcal{T} (\mathbf{A}^{\text{e}} + \alpha \mu \tan \beta) \boldsymbol{\lambda}^{\text{e}} \mathcal{L} \mathcal{L}^{\dagger} + \text{h.c.} \quad (31)$$

where

$$\mathbf{m}_L^2 = m_L^2 \mathbb{1}, \quad \mathbf{m}_e^2 = m_e^2 \mathbb{1} - \mathbf{I}_G, \quad \mathbf{A}^{\text{e}} = A_e \mathbb{1} - \frac{1}{3} \mathbf{I}'_G, \quad (32)$$

in a self-explanatory notation,

$$\mathcal{L}_{\mathcal{Y}} = \mathcal{Q}^{\text{T}} \boldsymbol{\lambda}_Z^{\text{u}} \mathcal{L}^{\dagger} \cdot \mathcal{L}^{\text{u}} + \mathcal{Q}^{\text{T}} \boldsymbol{\lambda}_Z^{\text{d}} \mathcal{L}^{\dagger} \cdot \mathcal{L}^{\text{d}} + \mathcal{L}^{\dagger} \mathcal{T} \boldsymbol{\lambda}_Z^{\text{e}} \mathcal{L} \cdot \mathcal{L}^{\text{d}} \quad (33)$$

where $\boldsymbol{\lambda}_Z^{\text{u}}$ has kept its diagonal form and the matrices $\boldsymbol{\lambda}^{\text{d}}$ and $\boldsymbol{\lambda}^{\text{e}}$, equal at M_G , have been shifted by the different renormalization effects due to λ_t and the gauge couplings. By diagonalizing $\boldsymbol{\lambda}_Z^{\text{d}}$ and $\boldsymbol{\lambda}_Z^{\text{e}}$, we have

$$\begin{aligned} \boldsymbol{\lambda}_Z^{\text{d}} v_{\text{d}} &= \mathbf{V}^* \mathbf{M}^{\text{d}} \mathbf{U}^{\dagger} \\ \boldsymbol{\lambda}_Z^{\text{e}} v_{\text{d}} &= \mathbf{V}^{\text{e}*} \mathbf{M}^{\text{e}} \mathbf{U}^{\text{e}\dagger} \end{aligned} \quad (34)$$

where \mathbf{M}^{d} , \mathbf{M}^{e} are the diagonal mass matrices for down quarks and charged leptons, $\mathbf{U} = \mathbf{U}^{\text{e}}$, \mathbf{V} is the usual Cabibbo-Kobayashi-Maskawa matrix and, as an effect of the top Yukawa coupling, the matrix elements of \mathbf{V}^{e} are related to those of \mathbf{V} by

$$V_{ij}^{\text{e}} = y V_{ij} \quad \text{for } i \neq j \text{ and } (i \text{ or } j) = 3, \quad V_{ij}^{\text{e}} = V_{ij} \quad \text{otherwise} \quad (35)$$

and y is defined in ref. [20].

We now switch to a mass eigenstate basis for the charged leptons:

$$\mathbf{V}^{\text{e}\dagger} e_L^c = e_L^c, \quad \mathbf{U}^{\text{e}\dagger} L = L'. \quad (36)$$

In order to keep neutral vertices diagonal in flavour space, we rotate sleptons simultaneously with leptons (we suppress primes after eq. (37)):

$$\mathbf{V}^{\text{e}\dagger} \tilde{e}_L^c = \tilde{e}_L^c, \quad \mathbf{U}^{\text{e}\dagger} \tilde{L} = \tilde{L}'. \quad (37)$$

This generates off-diagonal slepton mass terms:

$$\begin{aligned} (\delta_{ij}^l)_{RR} &= -\mathbf{V}_{3i}^{\text{e}*} \mathbf{V}_{3j}^{\text{e}} \frac{I_G}{m_l^2} \\ (\delta_{ij}^l)_{RL} &= -\frac{1}{3} \mathbf{V}_{3i}^{\text{e}} \mathbf{V}_{3j}^{\text{e}*} \frac{M_j^e I'_G}{m_{\tilde{l}}^2}, \end{aligned} \quad (38)$$

where we have defined as usual an average slepton mass $m_{\tilde{l}}$.

y	$ \left(\delta_{12}^l\right)_{RR} ^{ex}$	$ \left(\delta_{12}^l\right)_{RR} ^{th}$	$ \left(\delta_{12}^l\right)_{RL} ^{ex}$	$ \left(\delta_{12}^l\right)_{RL} ^{th}$
0.3	4.3×10^{-3}	1.8×10^{-4}	1.5×10^{-6}	1.0×10^{-7}
0.7	6.5×10^{-3}	1.5×10^{-4}	1.6×10^{-6}	1.1×10^{-7}
1.0	8.3×10^{-3}	1.2×10^{-4}	1.8×10^{-6}	1.2×10^{-7}

Table 10: Comparison between experimental limits $|\left(\delta_{ij}^l\right)_{AB}|^{ex}$ and values obtained in SU(5) for the δ 's. We have used $m_{\tilde{e}_R} = 100$ GeV, $\lambda_{tG} = 1.4$, $A_e/m_{\tilde{e}_R} = -1$, $\mu < 0$ and different values of $y = m_{\tilde{\gamma}}^2/m_{\tilde{e}_R}^2$.

y	$ \left(\delta_{12}^l\right)_{RR} \left(\delta_{22}^l\right)_{RL} ^{ex}$	$ \left(\delta_{12}^l\right)_{RR} \left(\delta_{22}^l\right)_{RL} ^{th}$ ($\tan \beta = 2$)	$ \left(\delta_{12}^l\right)_{RR} \left(\delta_{22}^l\right)_{RL} ^{th}$ ($\tan \beta = 10$)
0.3	2.6×10^{-6}	7.1×10^{-7}	2.2×10^{-6}
0.7	3.3×10^{-6}	7.5×10^{-7}	2.7×10^{-6}
1.0	4.5×10^{-6}	7.0×10^{-7}	2.6×10^{-6}

Table 11: Same as in table 10 for double mass insertions.

We now note that for large $\tan \beta$ it may be convenient to perform a Left-Right transition via a double mass insertion, a Left-Right flavour diagonal one $(\delta_{ii})_{LR} = M_i^e (A_e + \mu \tan \beta)/m_{\tilde{l}}^2$ followed by a Right-Right flavour changing one $(\delta_{ij})_{RR}$. Including this possibility one gets the following general expression for the decay $l_i \rightarrow l_j \gamma$: (see ref. [8]):

$$\begin{aligned}
 \text{BR}(l_i \rightarrow l_j \gamma) = & \frac{\alpha^3}{G_F^2} \frac{12\pi}{m_{\tilde{l}}^4} \left\{ \left| \left[M_3(x) + \frac{3}{2} (A_e + \mu \tan \beta) \frac{m_{\tilde{\gamma}}}{m_{\tilde{l}}^2} f_6(x) \right] \left(\delta_{ij}^l\right)_{LL} \right. \right. \\
 & \left. \left. + \frac{m_{\tilde{\gamma}}}{m_l} M_1(x) \left(\delta_{ij}^l\right)_{LR} \right|^2 + L \leftrightarrow R \right\} \cdot \text{BR}(l_i \rightarrow l_j \nu_i \bar{\nu}_j) . \quad (39)
 \end{aligned}$$

In tables 10 and 11, we compare the limits, obtained imposing that each individual term in eq. (39) does not exceed the value given in table 3, with the values predicted in SU(5).

5.2 SUSY SO(10)

Following the same procedure as in Section 5.1, one can derive the expression for the off-diagonal slepton mass terms. We maintain here the same notation as in Section 5.1, bearing in mind that the relations between low- and high-energy parameters have now changed (we refer again the reader to ref. [20] for details). One gets

$$\begin{aligned} (\delta_{ij}^l)_{LL} &= -\mathbf{V}_{3i}^e \mathbf{V}_{3j}^{e*} \frac{I_G}{m_{\tilde{l}}^2} \\ (\delta_{ij}^l)_{RR} &= -\mathbf{V}_{3i}^{e*} \mathbf{V}_{3j}^e \frac{I_G}{m_{\tilde{l}}^2} \\ (\delta_{ij}^l)_{LR} &= -\frac{5}{7} [\mathbf{V}_{3i}^e \mathbf{V}_{3j}^{e*} M_j^e + \mathbf{V}_{3i}^{e*} \mathbf{V}_{3j}^e M_i^e] \frac{I'_G}{m_{\tilde{l}}^2}. \end{aligned} \quad (40)$$

We now note that flavour violating terms which mediate the transition from flavour i to flavour j are always proportional to \mathbf{V}_{3i}^e and to \mathbf{V}_{3j}^e . Therefore, a $1 - 2$ transition must be proportional to $\mathbf{V}_{31}^{e*} \mathbf{V}_{32}^e$. On the other hand, an $i - 3$ transition is only proportional to \mathbf{V}_{3i}^e , as $\mathbf{V}_{33}^e = 1$. This means that a double mass insertion in which the intermediate flavour index is 3 is not suppressed with respect to a single insertion, as long as $I_G/m_{\tilde{l}}^2$ is of order one. In this case, by performing a double mass insertion, one can obtain an amplitude for the decay $\mu \rightarrow e\gamma$ which is proportional to m_τ instead of m_μ . If one takes this into account, the mass insertion method gives a good approximation of the complete result, whereas if one ignores the possibility of such double mass insertions, the method gives a poor approximation, as noted in ref. [20].

As in SU(5), in the large $\tan \beta$ region it may be convenient to perform a Left-Right transition via the flavour conserving $M^e (A_e + \mu \tan \beta)$ term, followed by an LL or RR flavour changing mass insertion. Hence, given that this latter term can be itself obtained by a double mass insertion, we end up with a competitive triple mass insertion. We have approximated the triple mass insertion by a double one with an *effective* Left-Right mass insertion given by

$$(\delta_{i3}^l)_{LR}^{effective} = (\delta_{i3}^l)_{LL} \times \frac{M_3^e (A_e + \mu \tan \beta)}{m_{\tilde{l}}^2}. \quad (41)$$

A comparison between experimental limits and theoretical predictions is given in tables 12 and 13.

y	$ \left(\delta_{12}^l\right)_{RR} ^{ex}$	$ \left(\delta_{12}^l\right)_{RR} ^{th}$	$ \left(\delta_{12}^l\right)_{RL} ^{ex}$	$ \left(\delta_{12}^l\right)_{RL} ^{th}$
0.1	2.8×10^{-2}	2.1×10^{-4}	4.7×10^{-6}	3.6×10^{-8}
0.3	3.9×10^{-2}	1.9×10^{-4}	4.4×10^{-6}	4.2×10^{-8}
0.7	6.0×10^{-2}	1.4×10^{-4}	5.0×10^{-6}	4.7×10^{-8}

Table 12: Comparison between experimental limits $|\left(\delta_{12}^l\right)_{AB}|^{ex}$ and values obtained in $SO(10)$ for the δ 's. In this case the model is $L - R$ symmetric, and limits are independent from the exchange $L \leftrightarrow R$. We have used $m_{\tilde{e}_R} = 300$ GeV, $\lambda_{tG} = 1.25$, $A_e/m_{\tilde{e}_R} = -1$, $\mu < 0$ and different values of $y = m_{\tilde{\gamma}}^2/m_{\tilde{e}_R}^2$.

y	$ \left(\delta_{13}^l\right)_{RR} \left(\delta_{32}^l\right)_{RL} ^{ex}$	$ \left(\delta_{13}^l\right)_{RR} \left(\delta_{32}^l\right)_{RL} ^{th}$	$ \left(\delta_{13}^l\right)_{RR} \left(\delta_{32}^l\right)_{RL}^{eff} ^{th}$ ($\tan \beta = 2$)	$ \left(\delta_{13}^l\right)_{RR} \left(\delta_{32}^l\right)_{RL}^{eff} ^{th}$ ($\tan \beta = 10$)
0.1	4.5×10^{-6}	1.8×10^{-5}	7.5×10^{-5}	1.9×10^{-4}
0.3	6.4×10^{-6}	1.3×10^{-5}	4.7×10^{-5}	1.5×10^{-4}
0.7	9.6×10^{-6}	7.2×10^{-6}	1.8×10^{-5}	6.4×10^{-5}

Table 13: Same as in table 12 for double mass insertions. In this case the relevant average slepton mass is defined as $m_{\tilde{l}} = \sqrt{m_{\tilde{e}_R} m_{\tilde{\tau}_R}}$. The last two columns contain effective insertions, as defined in the text.

5.3 Non-universal soft breaking terms

We now consider a simple model with minimal non-universality in the leptonic sector. Let us assume that the soft breaking terms for sleptons at the GUT scale M_G have the following form:

$$V_{\text{soft}} = \tilde{l}_L^\dagger \mathbf{m}_l^2 \tilde{l}_L + \tilde{e}_L^{c\dagger} \mathbf{m}_e^2 \tilde{e}_L^c + \tilde{e}_L^{cT} \mathbf{A}^1 \boldsymbol{\lambda}^1 \tilde{l}_L \bar{H}, \quad (42)$$

where

$$\begin{aligned} \mathbf{m}_l^2 &= \text{diag}(\tilde{m}_0^2 + \Delta_{m^2}, \tilde{m}_0^2, \tilde{m}_0^2 - \Delta_{m^2}) \\ \mathbf{m}_e^2 &= \tilde{m}_0^2 \mathbb{1} \\ \mathbf{A}^1 &= A_l \mathbb{1}. \end{aligned} \quad (43)$$

We now assume for simplicity that the Yukawa couplings of leptons are proportional to the ones of d -quarks in the basis where the couplings of u -quarks are diagonal. Performing the RGE evolution down to the electroweak scale, diagonalizing the lepton mass matrix and rotating sleptons to keep the $l - \tilde{l} - \tilde{\gamma}$ vertex diagonal, we get the flavour-violating mass insertion between selectrons and smuons

$$(\delta_{12}^l)_{LL} = (\mathbf{V}_{11}^1 \mathbf{V}_{12}^{1*} - \mathbf{V}_{13}^1 \mathbf{V}_{32}^{1*}) \frac{\Delta_{m^2}}{\tilde{m}^2} \simeq \mathbf{V}_{11} \mathbf{V}_{12}^* \frac{\Delta_{m^2}}{\tilde{m}^2}, \quad (44)$$

where \mathbf{V} is the CKM matrix and \tilde{m} is the low-energy slepton average mass. Starting from the limits in table 7 we obtain the constraints on $\delta_m = \Delta_{m^2}/\tilde{m}_0^2$ plotted in figure 13, as a function of $x = m_{\tilde{\gamma}}^2/m_{\tilde{l}}^2$. Notice that, differently from our previous discussion, here we restrict to the range $x < 0.5$. This is due to the fact that, as shown in ref. [22], the running of the mass parameters implies an upper bound on the ratio $m_{\tilde{\gamma}}^2/m_{\tilde{l}}^2$ at the electroweak scale of order 0.5.

If one compares the results plotted in fig. 13 with those in table 7, one finds that the ‘‘dilution’’ of the degeneracy constraint when going from the low to the large scale increases for a more accentuated gaugino dominance. Namely, the larger x is (compatibly with $x < 0.5$), the weaker is the constraint on δ_m .

6 Conclusions and outlook

In this paper we have provided a systematic study of all the most stringent constraints coming from FCNC and CP violating phenomena on the off-diagonal flavour-changing terms in the sfermion mass matrices. Our model-independent parameterization, which makes use of the mass-insertion method, is particularly suitable for a ready check of the

viability of any SUSY extension of the SM in view of the FCNC and CP tests. Obviously, such a kind of check can be considered only as a first, coarse approach to the full analysis of the FCNC and CP predictions within a specific SUSY model which requires the full diagonalization of the sfermion mass matrices. Needless to say, we think that the basic ignorance of the mechanism responsible for SUSY breaking and the consequent large variety of SUSY models in the context of supergravity and superstring theories make it necessary to have an adequate, preliminary test of the crucial FCNC and CP quantities readily available. Our analysis clarifies the extent to which the study of FCNC and CP via the mass insertion method is valid. In particular, the Section devoted to SUSY-GUT's makes it clear that a naive implementation of the method may lead to results which substantially differ from what is obtained in the “correct” mass eigenstate formalism.

A legitimate question that one can formulate at the end of such a long analysis is whether we can hope to find some indirect manifestation of SUSY through FCNC and CP violating phenomena and, if so, what are the best candidates. Obviously the answer is highly model-dependent. For instance, the MSSM might easily escape any kind of indirect manifestation through FCNC and/ or CP violation. On the other hand, SUSY-GUT's and models with non-universality have a high potentiality to produce FCNC and/or CP violating phenomena at a rate which is experimentally detectable. If a unification of leptons and quarks into common multiplets occurs, and if one can trust the use of RGE's in a delicate range such as that between M_{Pl} and M_{G} , then phenomena as $\mu \rightarrow e\gamma$ or $\mu - e$ conversion in atoms are the most likely candidates to exhibit some signal of new physics. In the sector of CP violation, as we have seen, if the δ_{LR} insertions are proportional to the Yukawa couplings of the d- and s-quarks, then $\delta_{LR} \ll \delta_{LL}$ and the SUSY contribution from gluino exchange is essentially of superweak nature. On the contrary, if one envisages the presence of a conspicuous δ_{LR} in the kaon system, then, while respecting the bound from ε , it is possible to obtain large SUSY contributions to ε'/ε . Notice, however, that $\text{Im}(\delta_{11}^d)_{LR}$ is strongly constrained by d_n (see table 9). Unless $\text{Im}(\delta_{12}^d)_{LR} \gg \text{Im}(\delta_{11}^d)_{LR}$ there is no hope for a sizeable SUSY contribution to ε'/ε even in models where the δ_{LR} quantities are not proportional to Yukawa couplings. Finally, B physics can be quite sensitive to the presence of gluino-mediated SUSY contributions. While the B oscillations can receive sizeable contributions both with or without a conspicuous δ_{LR} , this mass insertion is crucial if one asks for enhancement in the process $b \rightarrow s\gamma$ which requires a helicity flip. There is also a potentiality of conspicuous contributions to CP violation in B physics which has not been explored here.

In conclusion, our analysis confirms a twofold role played by FCNC and CP violating phenomena in shedding some light on the SUSY extensions of the SM. On one side, our

study emphasizes that the constraints coming from this class of processes are very severe and impose rather stringent selections of fundamental theories whose low energy limit is a SUSY extension of the SM. On the other hand, it emerges from our analysis that the bounds on the δ quantities that one derives from the available experimental data are not far from (or, even, clash with) the values for the δ 's that one finds in effective $N=1$ supergravities or SUSY-GUT's. In view of this latter observation, it is not unconceivable that, after all, SUSY may manifest itself through its contributions to FCNC and/or CP violating processes even before its direct discovery through the production of SUSY particles.

Acknowledgements

We thank R. Barbieri and R. Petronzio for useful discussions. Two of us (E.G. and L.S.) are grateful to the physics departments of Padova and Perugia for their kind hospitality during the completion of this work. E.G. would like to thank the theory division of CERN and the physics department of Southampton for their warm hospitality.

References

- [1] For a phenomenologically oriented review, see:
 P. Fayet and S. Ferrara, *Phys. Rep.* **32C** (1977) 249;
 H.P. Nilles, *Phys. Rep.* **110C** (1984) 1.
 For spontaneously broken $N=1$ supergravity, see:
 E. Cremmer, S. Ferrara, L. Girardello and A. Van Proeyen, *Nucl. Phys.* **B 212** (1983) 413 and references therein.
- [2] M. Dine, A. Kagan and S. Samuel, *Phys. Lett.* **B 243** (1990) 250;
 L. Ibáñez and D. Lüst, *Nucl. Phys.* **B 382** (1992) 305;
 V. Kaplunovsky and J. Louis, *Phys. Lett.* **B 306** (1993) 269;
 R. Barbieri, J. Louis and M. Moretti, *Phys. Lett.* **B 312** (1993) 451,
 (Erratum, *Phys. Lett.* **B 316** (1993) 632);
 B. de Carlos, J.A. Casas and C. Muñoz, *Phys. Lett.* **B 299** (1993) 234; *Nucl. Phys.* **B 399** (1993) 623;
 A. Brignole, L.E. Ibáñez and C. Muñoz, *Nucl. Phys.* **B 422** (1994) 125,
 (Erratum, *Nucl. Phys.* **B 436** (1995) 747);
 A. Lleyda and C. Muñoz, *Phys. Lett.* **B 317** (1993) 82;
 D. Matalliotakis and H.P. Nilles, *Nucl. Phys.* **B 435** (1995) 115;
 M. Olechowski and S. Pokorski, *Phys. Lett.* **B 344** (1995) 201;
 D. Choudhury, F. Eberlein, A. König, J. Louis and S. Pokorski, *Phys. Lett.* **B 342** (1995) 180;

P. Brax and M. Chemtob, *Phys. Rev.* **D 51** (1995) 6550;
 P. Brax, U. Ellwanger and C.A. Savoy, *Phys. Lett.* **B 347** (1995) 269;
 P. Brax and C.A. Savoy, *Nucl. Phys.* **B 447** (1995) 227.

[3] Y. Nir and N. Seiberg, *Phys. Lett.* **B 309** (1993) 337;
 M. Dine, R. Leigh and A. Kagan, *Phys. Rev.* **D 48** (1993) 4269;
 M. Leurer, Y. Nir and N. Seiberg, *Nucl. Phys.* **B 420** (1994) 468;
 R. Barbieri, G. Dvali and L.J. Hall, preprint LBL-38065 (December 1995), hep-ph/9512388.

[4] S. Dimopoulos, G.F. Giudice and N. Tetradis, *Nucl. Phys.* **B 454** (1995) 59.

[5] M. Dine, A.E. Nelson and Y. Shirman, *Phys. Rev.* **D 51** (1995) 1362;
 M. Dine, A.E. Nelson, Y. Nir and Y. Shirman, *Phys. Rev.* **D 53** (1996) 2658;
 S. Dimopoulos, M. Dine, S. Raby and S. Thomas, preprint SLAC-PUB-7104 (January 1996), hep-ph/9601367;
 G. Dvali, G.F. Giudice and A. Pomarol, CERN preprint CERN-TH-96-61 (March 1996), hep-ph/9603238;
 M. Lanzagorta and G.G. Ross, *Phys. Lett.* **B 364** (1995) 163.

[6] L.J. Hall, V.A. Kostelecky and S. Raby, *Nucl. Phys.* **B 267** (1986) 415.

[7] M.J. Duncan, *Nucl. Phys.* **B 221** (1983) 285;
 J.F. Donoghue, H.P. Nilles and D. Wyler, *Phys. Lett.* **B 128** (1983) 55.

[8] F. Gabbiani and A. Masiero, *Nucl. Phys.* **B 322** (1989) 235.

[9] J.S. Hagelin, S. Kelley and T. Tanaka, *Nucl. Phys.* **B 415** (1994) 293.

[10] E. Gabrielli, A. Masiero and L. Silvestrini, *Phys. Lett.* **B 374** (1996) 80.

[11] J.-M. Gérard, W. Grimus, A. Raychaudhuri and G. Zoupanos, *Phys. Lett.* **B 140** (1984) 349.

[12] G. Beall, M. Bander and A. Soni, *Phys. Rev. Lett.* **48** (1982) 848.

[13] P. Langacker and R. Sathiapalan, *Phys. Lett.* **B 144** (1984) 401;
 J.-M. Gérard, W. Grimus and A. Raychaudhuri, *Phys. Lett.* **B 145** (1984) 400;
 M. Dugan, B. Grinstein and L. Hall, *Nucl. Phys.* **B 255** (1985) 413;
 L.J. Hall, V.A. Kostelecky and S. Raby, *Nucl. Phys.* **B 267** (1986) 415;
 J.S. Hagelin and L.S. Littenberg, *Prog. Part. Nucl. Phys.* **23** (1989) 1;
 E. Gabrielli and G. Giudice, *Nucl. Phys.* **B 433** (1995) 3.

[14] A.J. Buras, M. Jamin and M.E. Lautenbacher, *Nucl. Phys.* **B 408** (1993) 209;
 M. Ciuchini, E. Franco, G. Martinelli and L. Reina, in The Second Daphne Physics Handbook, L. Maiani, G. Pancheri and N. Paver, eds., p.27.

[15] S. Bertolini, F. Borzumati, A. Masiero and G. Ridolfi, *Nucl. Phys.* **B 353** (1991) 591.

- [16] S. Bertolini, F. Borzumati and A. Masiero, *Phys. Rev. Lett.* **59** (1987) 180; N.G. Deshpande, P. Lo, J. Trampetic, G. Eilam and P. Singer, *Phys. Rev. Lett.* **59** (1987) 183; B. Grinstein, R. Springer and M.B. Wise, *Phys. Lett.* **B 202** (1988) 138; *Nucl. Phys.* **B 339** (1990) 269; M. Ciuchini, E. Franco, G. Martinelli, L. Reina and L. Silvestrini, *Phys. Lett.* **B 316** (1993) 127; M. Ciuchini, E. Franco, L. Reina and L. Silvestrini, *Nucl. Phys.* **B 421** (1994) 41.
- [17] A.J. Buras, M. Misiak, M. Munz and S. Pokorski, *Nucl. Phys.* **B 424** (1994) 374.
- [18] M.A. Diaz, *Phys. Lett.* **B 304** (1993) 278; N. Oshimo, *Nucl. Phys.* **B 404** (1993) 20; R. Barbieri and G.F. Giudice, *Phys. Lett.* **B 309** (1993) 86; Y. Okada, *Phys. Lett.* **B 315** (1993) 119; R. Garisto and J.N. Ng, *Phys. Lett.* **B 315** (1993) 372; F. Borzumati, *Zeit. für Physik* **C 63** (1994) 291; S. Bertolini and F. Vissani, *Zeit. für Physik* **C 67** (1995) 513.
- [19] R. Barbieri and L.J. Hall, *Phys. Lett.* **B 338** (1994) 212.
- [20] R. Barbieri, L.J. Hall and A. Strumia, *Nucl. Phys.* **B 445** (1995) 219.
- [21] R. Barbieri, L.J. Hall and A. Strumia, *Nucl. Phys.* **B 449** (1995) 437; N. Arkani-Hamed, H.-C. Cheng and L.J. Hall, preprint LBL-37343, August 1995, hep-ph/9508288.
- [22] D. Choudhury, F. Eberlein, A. König, J. Louis and S. Pokorski, in ref. [2].

Figure 1: Feynman diagrams for $\Delta S = 2$ transitions, with $h, k, l, m = \{L, R\}$.

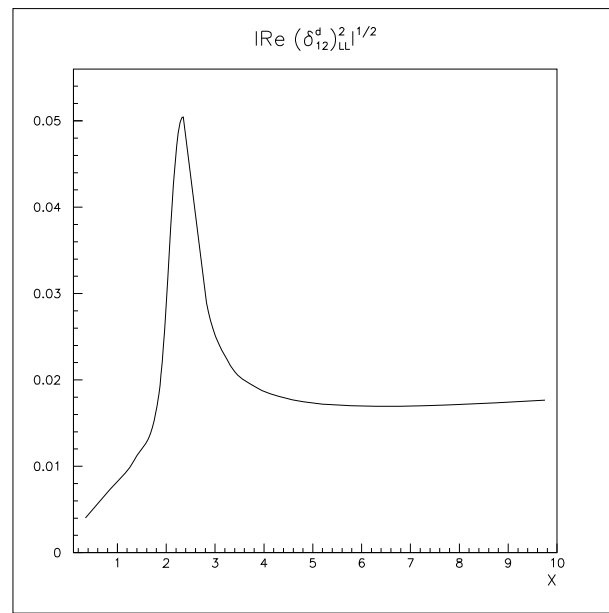


Figure 2: The $\sqrt{\left| \text{Re} \left(\delta_{12}^d \right)_{LL}^2 \right|}$ as a function of $x = m_{\tilde{g}}^2/m_{\tilde{q}}^2$, for an average squark mass $m_{\tilde{q}} = 100 \text{ GeV}$.

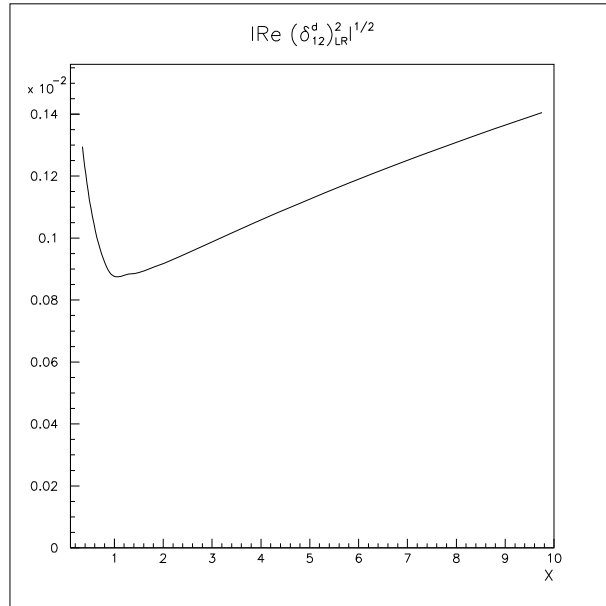


Figure 3: The $\sqrt{|\text{Re}(\delta_{12}^d)^2_{LR}|}$ as a function of $x = m_{\tilde{g}}^2/m_{\tilde{q}}^2$, for an average squark mass $m_{\tilde{q}} = 100\text{GeV}$.

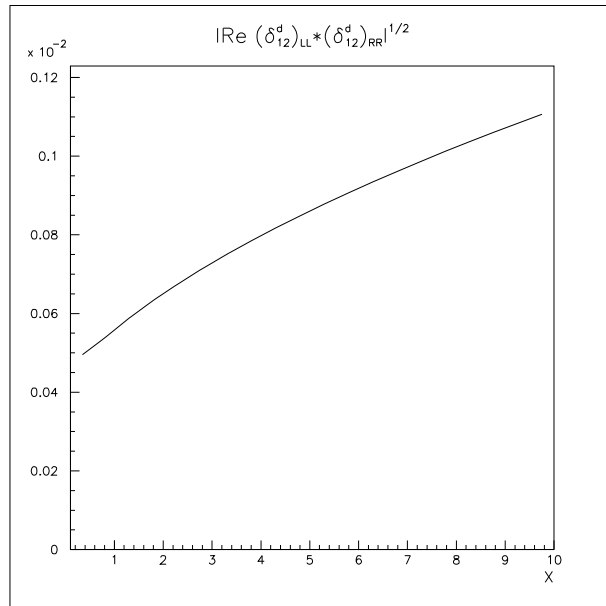


Figure 4: The $\sqrt{|\text{Re}(\delta_{12}^d)^2_{LL} (\delta_{12}^d)^2_{RR}|}$ as a function of $x = m_{\tilde{g}}^2/m_{\tilde{q}}^2$, for an average squark mass $m_{\tilde{q}} = 100\text{GeV}$.

Figure 5: Box diagrams for $\Delta S = 1$ transitions, with $h, k, m = \{L, R\}$.

Figure 6: Penguin diagrams for $\Delta S = 1$ transitions, with $h, k = \{L, R\}$.

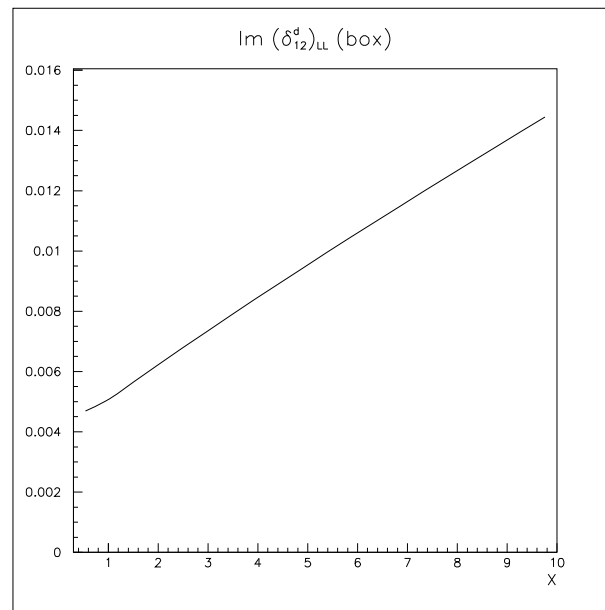


Figure 7: The $\text{Im} (\delta_{12}^d)_{LL}$ as a function of $x = m_{\tilde{g}}^2/m_{\tilde{q}}^2$, obtained considering only the box contribution, for an average squark mass $m_{\tilde{q}} = 100\text{GeV}$.

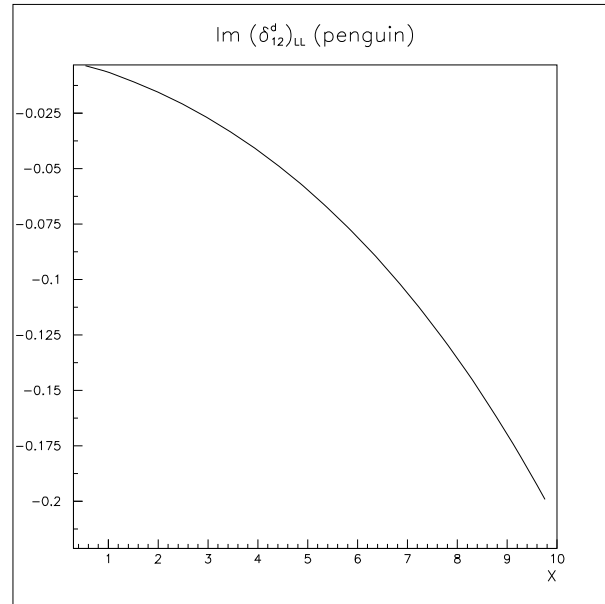


Figure 8: The $\text{Im}(\delta_{12}^d)_{LL}$ as a function of $x = m_{\tilde{g}}^2/m_{\tilde{q}}^2$, obtained considering only the penguin contribution, for an average squark mass $m_{\tilde{q}} = 100\text{GeV}$.

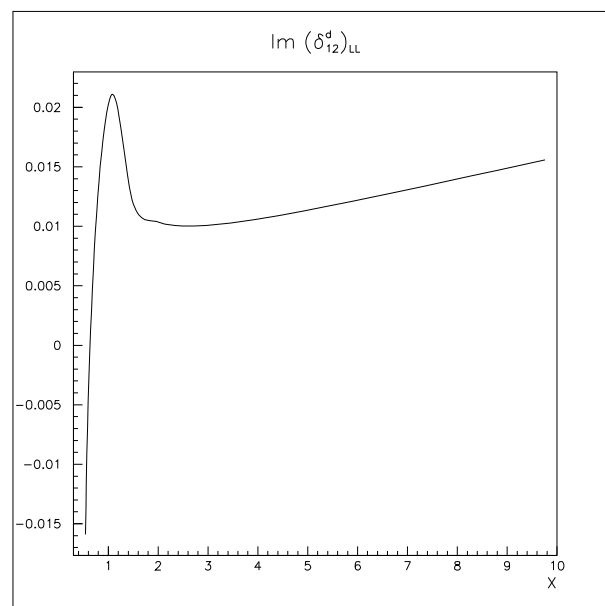


Figure 9: The $\text{Im}(\delta_{12}^d)_{LL}$ as a function of $x = m_{\tilde{g}}^2/m_{\tilde{q}}^2$, for an average squark mass $m_{\tilde{q}} = 100\text{GeV}$.

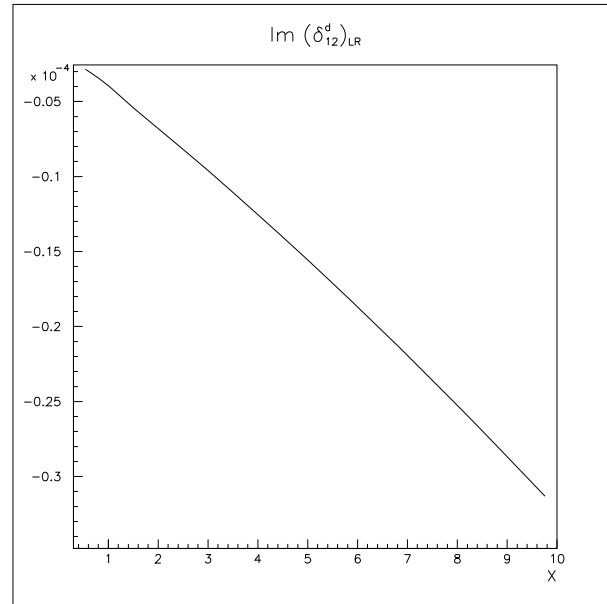


Figure 10: The $\text{Im}(\delta_{12}^d)_{LR}$ as a function of $x = m_{\tilde{g}}^2/m_{\tilde{q}}^2$, for an average squark mass $m_{\tilde{q}} = 100\text{GeV}$.

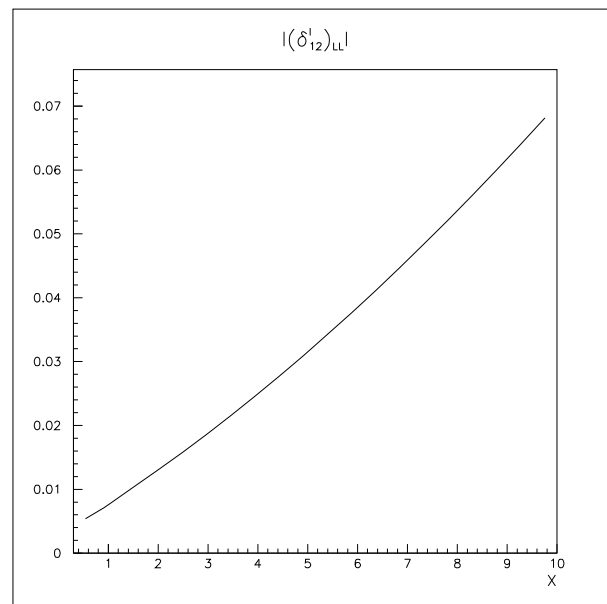


Figure 11: The $|(δ_{12}^l)_{LL}|$ as a function of $x = m_{\tilde{\gamma}}^2/m_{\tilde{l}}^2$, for an average slepton mass $m_{\tilde{l}} = 100\text{GeV}$.

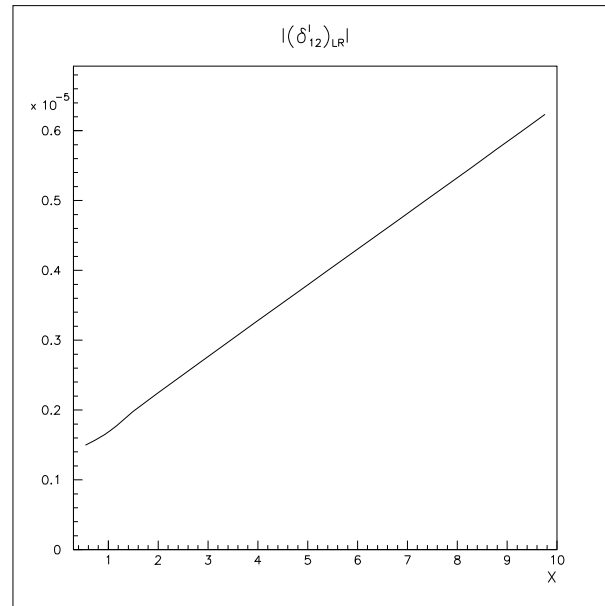


Figure 12: The $|\left(\delta_{12}^l\right)_{LR}|$ as a function of $x = m_{\tilde{\gamma}}^2/m_{\tilde{l}}^2$, for an average slepton mass $m_{\tilde{l}} = 100\text{GeV}$.

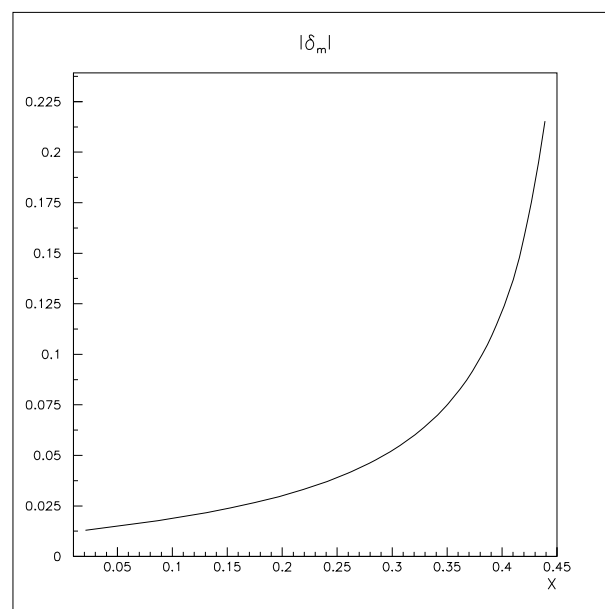
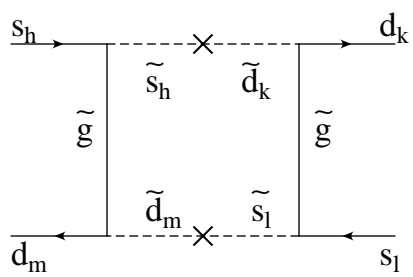
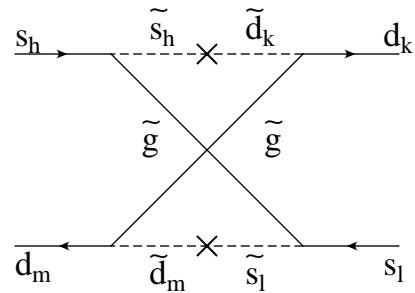


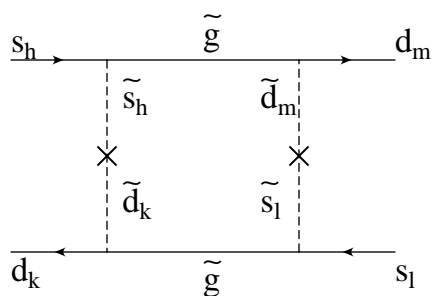
Figure 13: The $|\delta_m|$ as a function of $x = m_{\tilde{\gamma}}^2/m_{\tilde{l}}^2$, for an average slepton mass $m_{\tilde{l}} = 100\text{GeV}$.



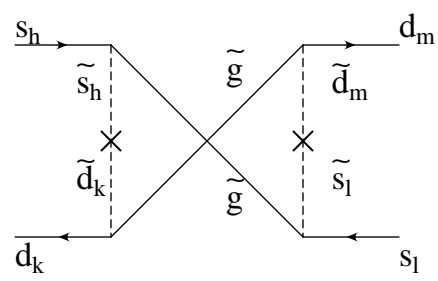
a)



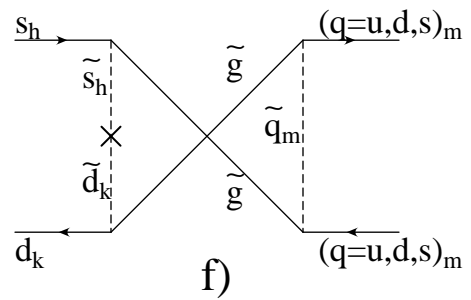
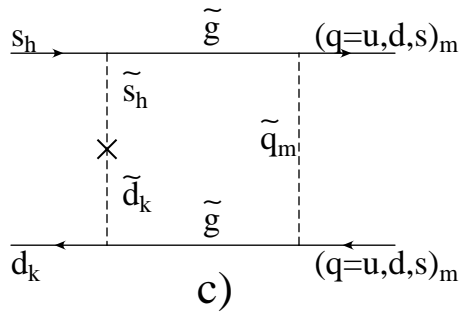
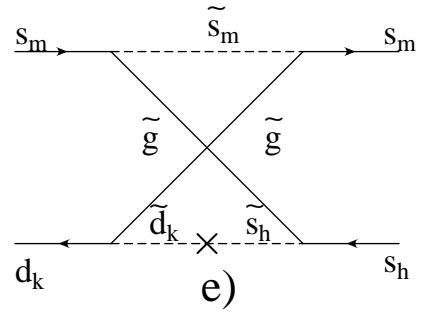
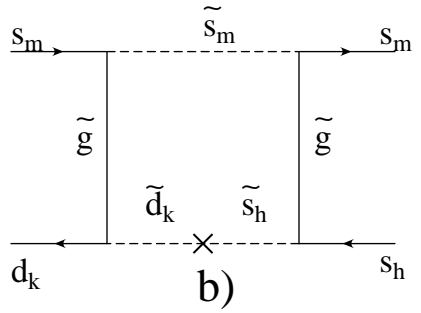
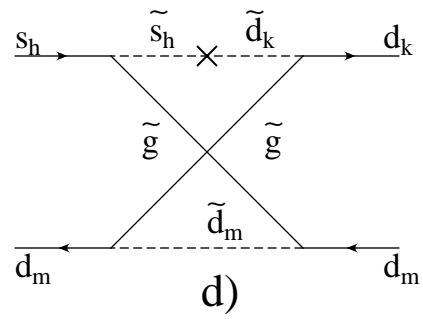
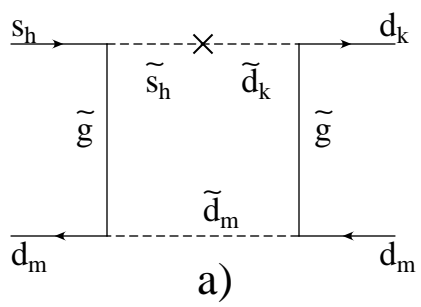
c)

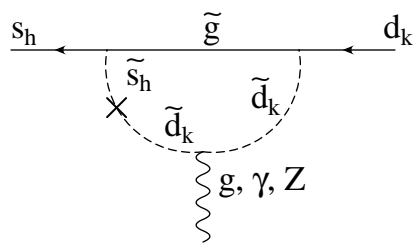


b)

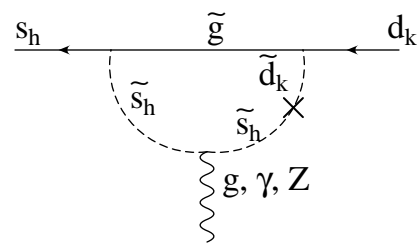


d)

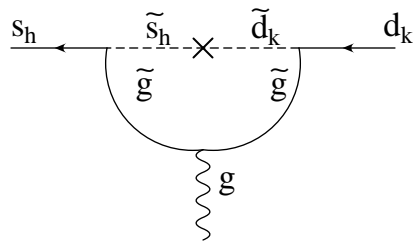




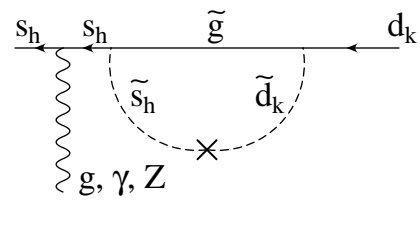
a)



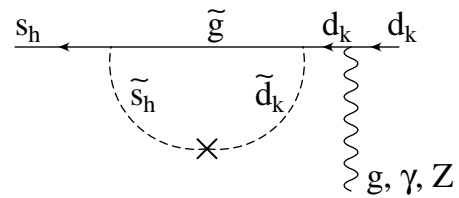
b)



c)



d)



e)